10.48047/jocaaa.2025.34.09.04

A nonstandard Finite Difference Approach Preserving Dynamic Consistency ForPredator–Prey Systems

Ali Youssef Musa
Email: alialjebory19981215@gmail.com

Abstract

We develop a nonstandard finite–difference (NSFD) approach for predator–prey systems that preserves dynamic consistency with their continuous counterparts. Focusing on models with a Holling type-III functional response, the discrete scheme is constructed so that fundamental qualitative features are retained for any time step: solutions remain positive and uniformly bounded, and population persistence is ensured. We characterize all equilibria of the continuous model and of the induced discrete map, and we prove that the stability type is inherited by the discretization. In particular, an interior equilibrium of the differential system may generate a Hopf bifurcation, while the corresponding fixed point of the NSFD map exhibits a Neimark–Sacker bifurcation under analogous parameter conditions. Numerical experiments corroborate the analysis and illustrate the robustness of the proposed method compared with standard schemes.

Keywords: Predator–prey dynamics; nonstandard finite difference; dynamic consistency; positivity and boundedness; persistence; equilibrium stability; Neimark–Sacker bifurcation

Introduction

Predator–prey interactions serve as canonical testbeds for understanding nonlinear ecological dynamics, including stability, oscillations, and coexistence [1,4]. Discrete-time formulations are especially appropriate when generations do not overlap or when observations occur at fixed sampling intervals, making them natural surrogates for many field and laboratory settings [1]. However, naïve discretizations (e.g., forward Euler) may generate spurious artifacts—negative populations, artificial equilibria, or step-size–dependent instabilities—thereby breaking dynamic consistency with the parent differential equations [1,4,5].

10.48047/jocaaa.2025.34.09.04

Nonstandard finite difference (NSFD) methods address these issues by replacing the step size with problem-dependent denominator functions and by using nonlocal representations of nonlinear terms, which together preserve qualitative invariants for broad step-size ranges [3,12,7].

Within predator–prey modeling, NSFD schemes have repeatedly been shown to maintain positivity, boundedness, and persistence while preserving the location and type of equilibria in the discrete model [1,3,11].

A hallmark observation is that when a continuous model experiences a Hopf bifurcation at an interior equilibrium, an appropriately designed NSFD discretization exhibits a Neimark–Sacker bifurcation at the corresponding fixed point, faithfully mirroring the onset of quasi-periodic oscillations in discrete time [1,5,6].

Recent work has pushed NSFD accuracy beyond first order by combining nonlocal reconstructions with modified denominator functions, yielding second-order convergence while retaining dynamical consistency [2,8].

These advances enable robust simulation of widely used predator–prey families—such as Rosenzweig–MacArthur—at step sizes that typically destabilize standard integrators [2,3]. NSFD ideas have also been extended to delayed predator–prey dynamics, where discrete maps derived from delay differential equations preserve equilibrium stability, capture stability switching, and reproduce Neimark–Sacker transitions [10].

Beyond ODE settings, NSFD methodology is being adapted to spatial predator–prey models with diffusion or cross-diffusion, where positivity and stability constraints are delicate and structure-preserving schemes demonstrate clear advantages over standard methods [9,7].

Collectively, this literature points to two priorities for discretizing ecological dynamics: preservation of qualitative structure (positivity, boundedness, invariant sets) and fidelity of local bifurcations across time scales, both of which are central to reliable inference and control design in discrete models [1–3,7]. Motivated by these developments, the present study proposes a nonstandard finite difference framework that enforces dynamic consistency for general predator–prey systems, establishes positivity, boundedness, and persistence, matches continuous-time equilibrium stability/bifurcation (Hopf ↔ Neimark–Sacker), and

10.48047/jocaaa.2025.34.09.04

validates accuracy and robustness against standard schemes through targeted numerical experiments [1–3].

Materials and Methods

Dynamics of System

We begin by establishing positivity, uniform bounds, and permanence for solutions of system (1) with strictly positive initial data. Throughout we assume $r, k, \alpha, \beta, s, h > 0$.

[Positivity, boundedness, permanence] Let $(x(0), y(0)) = (x_0, y_0) \in (0, \infty)^2$. Then:

1. **Positivity and positive invariance.** Writing the equations in separated form,

$$\frac{x'(t)}{x(t)} = r\left(1 - \frac{x(t)}{k}\right) - \frac{\alpha\, x(t)\, y(t)}{x(t)^2 + \beta^2}, \qquad \frac{y'(t)}{y(t)} = s\left(1 - \frac{h\, y(t)}{x(t)}\right).$$

Hence

$$x(t) = x_0 \exp\left(\int_0^t \left[r\left(1 - \frac{x(\xi)}{k}\right) - \frac{\alpha\, x(\xi)\, y(\xi)}{x(\xi)^2 + \beta^2}\right] d\xi\right) > 0, \quad y(t) = y_0 \exp\left(\int_0^t s\left(1 - \frac{h\, y(\xi)}{x(\xi)}\right) d\xi\right) > 0.$$

Thus the positive quadrant $\mathcal{S} := \{(x, y) : x > 0,\ y > 0\}$ is positively invariant; solutions starting in $\mathcal{S}$ remain in $\mathcal{S}$ for all $t \geq 0$.

2. **A priori upper bounds.** Using $y \geq 0$ in the prey equation,

$$x'(t) \leq r\, x(t)\left(1 - \frac{x(t)}{k}\right),$$

and comparison with the logistic equation yields $x(t) \leq \bar{x} := \max\{x_0, k\}$ for all $t \geq 0$. Then

$$y'(t) \leq s\, y(t)\left(1 - \frac{h\, y(t)}{\bar{x}}\right),$$

so $y(t) \leq \bar{y} := \max\{y_0, \bar{x}/h\}$ for all $t \geq 0$. In particular,

10.48047/jocaaa.2025.34.09.04

$$\limsup_{t\to\infty} x(t) \le k, \qquad \limsup_{t\to\infty} y(t) \le \frac{k}{h}.$$

3. **Permanence.** If

$$\alpha\, k^2 < r\, h\, \beta^2,$$

then there exist $m_x, m_y > 0$ (independent of initial data) such that $\liminf_{t\to\infty} x(t) \ge m_x$ and $\liminf_{t\to\infty} y(t) \ge m_y$. Indeed, from the prey equation and the bounds above,

$$x'(t) \ge x(t)[r\left(1 - \frac{x(t)}{k}\right) - \frac{\alpha k^2}{h\beta^2}],$$

which implies

$$\liminf_{t\to\infty} x(t) \ge m_x := k(1 - \frac{\alpha k^2}{rh\beta^2}) > 0.$$

Substituting this into the predator equation gives

$$y'(t) \ge s\, y(t)(1 - \frac{h\, y(t)}{m_x}),$$

and hence $\liminf_{t\to\infty} y(t) \ge m_y := \frac{m_x}{h} > 0$.

Equilibria and nullclines

The zero–growth sets are

$$x[r\left(1 - \frac{x}{k}\right) - \frac{\alpha x\, y}{x^2+\beta^2}] = 0, \qquad y(1 - \frac{h\, y}{x}) = 0.$$

Thus there is always the boundary equilibrium $E_0 = (k, 0)$. Any interior equilibrium $E_* = (x_*, y_*) \in \mathcal{S}$ must satisfy

$$y_* = \frac{x_*}{h}, \qquad r\left(1 - \frac{x_*}{k}\right) = \frac{\alpha x_*\, y_*}{x_*^2+\beta^2}.$$

Eliminating y_* yields the cubic

$$x_*^3 + a\, x_*^2 + \beta^2 x_* - k\beta^2 = 0, \qquad a := \frac{(\alpha - hr)k}{hr}.$$

10.48047/jocaaa.2025.34.09.04

The function $f(x) := r(1 - x/k) - \frac{\alpha x^2}{h(x^2+\beta^2)}$ is strictly decreasing on $(0, \infty)$, with $f(0^+) = r > 0$ and $f(x) \to -\infty$ as $x \to \infty$; hence there is a *unique* $x_* > 0$ solving $f(x_*) = 0$, and $y_* = x_*/h > 0$.

Local behavior at equilibria

Let $F = (F_1, F_2)$ denote the right–hand side of (1). The Jacobian at a point (x, y) is

$$J(x,y) = \begin{pmatrix} r(1-2x/k) - \frac{2\alpha x\beta^2 y}{(x^2+\beta^2)^2} & -\frac{\alpha x^2}{x^2+\beta^2} \\ sh\,\frac{y^2}{x^2} & s\left(1 - 2\frac{hy}{x}\right) \end{pmatrix}.$$

Boundary state $E_0 = (k, 0)$.

$$J(E_0) = \begin{pmatrix} -r & -\frac{\alpha k^2}{k^2+\beta^2} \\ 0 & s \end{pmatrix},$$

whose eigenvalues are $-r < 0$ and $s > 0$; thus E_0 is a *saddle*.

Interior state $E_* = (x_*, y_* = x_*/h)$.

$$\partial_x F_1(E_*) = r\left(1 - \frac{2x_*}{k}\right) - \frac{2\alpha x_*\beta^2 y_*}{(x_*^2+\beta^2)^2}, \quad \partial_y F_1(E_*) = -\frac{\alpha x_*^2}{x_*^2+\beta^2},$$

$$\partial_x F_2(E_*) = \frac{s}{h}, \qquad \partial_y F_2(E_*) = -s.$$

Hence

10.48047/jocaaa.2025.34.09.04

$$trJ(E_*) = [r - \frac{2rx_*}{k} - \frac{2\alpha\beta^2 x_* y_*}{(x_*^2+\beta^2)^2}] - s, \qquad \det J(E_*) = -s\,\partial_x F_1(E_*) + \frac{s\alpha x_*^2}{h(x_*^2+\beta^2)}.$$

Since $y_* = x_*/h$ and E_* satisfies the prey nullcline, one checks that $\det J(E_*) > 0$. Consequently, E_* is locally asymptotically stable iff $trJ(E_*) < 0$.

Hopf threshold

Because $\frac{d}{ds} trJ(E_*) = -1 \neq 0$, varying the predator growth parameter s transversely drives the trace through zero while $\det J(E_*) > 0$. The critical value is

$$s_0 := r - \frac{2rx_*}{k} - \frac{2\alpha\beta^2 x_* y_*}{(x_*^2+\beta^2)^2} = r - \frac{2rx_*}{k} - \frac{2\alpha\beta^2 x_*^2}{h\,(x_*^2+\beta^2)^2},$$

at which $J(E_*)$ has a pair of purely imaginary eigenvalues. Under the usual nondegeneracy and transversality conditions, the system undergoes a *Hopf bifurcation* at $s = s_0$.

[On period–doubling] System (1) is a continuous-time flow; period-doubling ("flip") is not a local equilibrium bifurcation in flows. The relevant codimension-one oscillatory instability is the Hopf bifurcation identified above.

We now turn to the discrete NSFD formulation (3) with step size $\delta > 0$. Throughout, parameters satisfy $r, k, \alpha, \beta, s, h > 0$.

[Permanence for the discrete model] Assume $\alpha k^2 < rh\beta^2$. Then every solution $\{(x_n, y_n)\}_{n\geq 0}$ of (3) with $x_0 > 0$, $y_0 > 0$ is positive, uniformly bounded, and permanent: there exist $m_x, m_y > 0$ such that

$$\liminf_{n\to\infty} x_n \geq m_x, \qquad \liminf_{n\to\infty} y_n \geq m_y.$$

Proof. Positivity and upper bounds. From the update rules of (3) one has for all $n \geq 0$,

10.48047/jocaaa.2025.34.09.04

$$x_{n+1} = \frac{(1+\delta r)\, x_n}{1+\frac{\delta r}{k} x_n + \frac{\alpha\delta\, x_n y_n}{x_n^2+\beta^2}} \;\le\; \frac{(1+\delta r)\, x_n}{1+\frac{\delta r}{k} x_n},$$

which by comparison with the logistic rational map yields $x_n \le \bar{x} := \max\{x_0, k\}$ for all n. Similarly,

$$y_{n+1} = \frac{(1+s\delta)\, y_n}{1+s\delta \frac{h y_n}{x_n}} \;\le\; \frac{(1+s\delta)\, y_n}{1+s\delta \frac{h y_n}{\bar{x}}},$$

and hence $y_n \le \bar{y} := \max\{y_0, \bar{x}/h\}$ for all n. In particular, $\limsup_{n\to\infty} x_n \le k$ and $\limsup_{n\to\infty} y_n \le k/h$.

Lower bounds (permanence). Using the bounds above and $x_n^2 + \beta^2 \ge \beta^2$,

$$x_{n+1} = \frac{(1+\delta r)\, x_n}{1+\frac{\delta r}{k} x_n + \frac{\alpha\delta\, x_n y_n}{x_n^2+\beta^2}} \;\ge\; \frac{(1+\delta r)\, x_n}{1+\frac{\delta r}{k} x_n + \frac{\alpha\delta\, k^2}{h\beta^2}}.$$

A standard comparison then gives

$$\liminf_{n\to\infty} x_n \;\ge\; m_x := k\left(1 - \frac{\alpha k^2}{r h \beta^2}\right) > 0.$$

Substituting this into the predator update produces

$$y_{n+1} \;\ge\; \frac{(1+s\delta)\, y_n}{1+s\delta \frac{h y_n}{m_x}} \quad\Rightarrow\quad \liminf_{n\to\infty} y_n \;\ge\; m_y := \frac{m_x}{h} > 0.$$

This proves permanence.

Fixed points and linearization

The fixed points of (3) are determined by the zero–growth relations

$$x\left[r\left(1 - \frac{x}{k}\right) - \frac{\alpha x y}{x^2+\beta^2}\right] = 0, \qquad y\left(1 - \frac{hy}{x}\right) = 0.$$

Hence the boundary fixed point $E_0 = (k, 0)$ is always present; any interior fixed point $E_* = (x_*, y_*)$ satisfies $y_* = \frac{x_*}{h}$ and $r\left(1 - \frac{x_*}{k}\right) = \frac{\alpha x_* y_*}{x_*^2+\beta^2}$. Introduce $Q := x_*^2 + \beta^2$ for brevity.

Let $V(x, y) = D\Phi_\delta(x, y)$ denote the variational matrix of the one–step map Φ_δ of (3).

10.48047/jocaaa.2025.34.09.04

Boundary fixed point $E_0 = (k, 0)$.

A direct differentiation gives an upper–triangular Jacobian

$$V(E_0) = \begin{pmatrix} \frac{1-\delta r}{1+\delta r} & -\frac{\alpha\delta\, k^2}{(k^2+\beta^2)(1+\delta r)} \\ 0 & 1+s\delta \end{pmatrix}.$$

Thus the eigenvalues are $\lambda_1 = \frac{1-\delta r}{1+\delta r}$ and $\lambda_2 = 1 + s\delta$. Since $|\lambda_1| < 1$ and $|\lambda_2| > 1$ for $r, \delta, s > 0$, E_0 is a saddle.

Interior fixed point $E_* = (x_*, y_* = \frac{x_*}{h})$.

After simplifying derivatives using the fixed–point identities, one can write

$$V(E_*) = \begin{pmatrix} \frac{1}{1+\delta r}\left(1 + \frac{2\alpha\delta\, x_*^3 y_*}{Q^2}\right) & -\frac{\alpha\delta\, x_*^2}{(1+\delta r)\, Q} \\ \frac{s\delta}{h(1+s\delta)} & \frac{1}{1+s\delta} \end{pmatrix}.$$

Let $\tau = trV(E_*)$ and $\Delta = \det V(E_*)$. Then the characteristic polynomial is

$$P(\lambda) = \lambda^2 - \tau\,\lambda + \Delta,$$

with

$$\tau = \frac{1}{1+\delta r}\left(1 + \frac{2\alpha\delta\, x_*^3 y_*}{Q^2}\right) + \frac{1}{1+s\delta}, \qquad \Delta = \frac{s\alpha\delta^2 x_*^2 Q + h(Q^2 + 2\alpha\delta\, x_*^3 y_*)}{h\, Q^2(1+\delta r)(1+s\delta)}.$$

Jury conditions and stability test

For a two–dimensional discrete system, local asymptotic stability is equivalent to the three Jury inequalities:

$$P(1) = 1 - \tau + \Delta > 0, \qquad P(-1) = 1 + \tau + \Delta > 0, \qquad 1 - \Delta > 0.$$

Using $y_* = \frac{x_*}{h}$ and $Q = x_*^2 + \beta^2$, a direct computation yields

10.48047/jocaaa.2025.34.09.04

$$P(1) = \frac{s\delta^2(\alpha x_*^2 Q + h(rQ^2 - 2\alpha x_*^3 y_*))}{h\,Q^2(1+\delta r)(1+s\delta)}.$$

Since

$$rQ^2 - 2\alpha x_*^3 y_* = r(x_*^2 + \beta^2)^2 - \frac{2\alpha}{h}x_*^4 = (hr - \alpha)\frac{x_*^4}{h} + 2r\beta^2 x_*^2 + r\beta^4,$$

we have $P(1) > 0$ whenever $\alpha < hr$. Moreover, one finds

$$P(-1) = \frac{s\alpha\delta^2 x_*^2 Q + h(2+s\delta)(2Q^2 + \delta(2\alpha x_*^3 y_* + rQ^2))}{h\,Q^2(1+\delta r)(1+s\delta)} \;>\; 0,$$

so the "flip" (period–doubling) condition is not met at E_*.

Finally,

$$\Delta < 1 \quad \Leftrightarrow \quad s\alpha\delta^2 x_*^2 Q + h(Q^2 + 2\alpha\delta x_*^3 y_*) < h\,Q^2(1+\delta r)(1+s\delta).$$

Assume $\alpha < hr$. If, in addition,

$$s\alpha\delta^2 x_*^2 Q + h(Q^2 + 2\alpha\delta x_*^3 y_*) < h\,Q^2(1+\delta r)(1+s\delta),$$

then the unique positive fixed point $E_* = (x_*, x_*/h)$ of (3) is locally asymptotically stable.

[Exclusion of period–doubling] Since $P(-1) > 0$ at E_*, the Jury criterion for a flip bifurcation fails; hence no period–doubling occurs at the interior fixed point under the stated hypotheses. The generic oscillatory loss of stability, if it occurs, is therefore via a Neimark–Sacker bifurcation.

Neimark–Sacker (discrete Hopf) bifurcation

We investigate the onset of a closed invariant curve at the interior fixed point $E_* = (x_*, y_*)$ of the NSFD map associated with system (3). Treat the predator intrinsic parameter s as the bifurcation parameter and write the one–step map

$$\Phi_\delta : (u, v) \mapsto \left(\frac{(1+\delta r)\,u}{1+\frac{\delta r}{k}u+\frac{\alpha\delta\,uv}{u^2+\beta^2}},\ \frac{(1+s\delta)\,v}{1+s\delta\frac{hv}{u}}\right). \qquad (1)$$

At an interior fixed point $E_* = (x_*, y_*)$ of (1) we have $y_* = x_*/h$ and set

10.48047/jocaaa.2025.34.09.04

$$Q := x_*^2 + \beta^2.$$

The Jacobian $V(E_*; s) = D\Phi_\delta(E_*; s)$ is

$$V(E_*; s) = \begin{pmatrix} \frac{1}{1+\delta r}\left(1 + \frac{2\alpha\delta\, x_*^3 y_*}{Q^2}\right) & -\frac{\alpha\delta\, x_*^2}{(1+\delta r)\, Q} \\ \frac{s\delta}{h\,(1+s\delta)} & \frac{1}{1+s\delta} \end{pmatrix}. \qquad (2)$$

Let

$$\tau(s) := trV(E_*; s), \qquad \Delta(s) := \det V(E_*; s).$$

From (2) one obtains

$$\tau(s) = \frac{1}{1+\delta r}\left(1 + \frac{2\alpha\delta\, x_*^3 y_*}{Q^2}\right) + \frac{1}{1+s\delta}, \qquad \Delta(s) = \frac{s\,\alpha\delta^2 x_*^2 Q + h(Q^2 + 2\alpha\delta\, x_*^3 y_*)}{h\, Q^2(1+\delta r)(1+s\delta)}. \qquad (3)$$

Crossing the unit circle.

A Neimark–Sacker (NS) bifurcation occurs when the complex conjugate eigenvalues of $V(E_*; s)$ cross the unit circle. This happens at $s = s_1$ satisfying

$$\Delta(s_1) = 1 \quad \Leftrightarrow \quad s_1 = \frac{h(rQ^2 - 2\alpha x_*^3 y_*)}{\alpha\delta\, x_*^2 Q - hQ^2(1+\delta r)}, \quad (4)$$

provided the denominator in (4) is nonzero. Nonresonance at the crossing requires

$$-2 < \tau(s_1) < 2, \qquad (5)$$

so that the eigenvalues are not equal to ± 1 at the onset. Transversality is guaranteed by

$$\frac{d}{ds}\,|\lambda(s)||_{s=s_1} = \frac{1}{2}\,\frac{d\Delta}{ds}|_{s=s_1} = \frac{\delta(\alpha\delta\, x_*^2 Q - hQ^2(1+\delta r))}{2\,h\,Q^2(1+\delta r)\,(1+s_1\delta)} \neq 0, \qquad (6)$$

which is equivalent to the same nonvanishing denominator as in (4).

Centering and Taylor expansion.

Set $s = s_1 + \tilde{s}$ and shift the fixed point to the origin:

$$x := u - x_*, \qquad y := v - y_*.$$

The map (1) becomes

10.48047/jocaaa.2025.34.09.04

$$\begin{pmatrix} x_{n+1} \\ y_{n+1} \end{pmatrix} = A(\tilde{s}) \begin{pmatrix} x_n \\ y_n \end{pmatrix} + \begin{pmatrix} f(x_n, y_n) \\ g(x_n, y_n) \end{pmatrix}, \qquad A(\tilde{s}) = V(E_*; s_1 + \tilde{s}), \qquad (7)$$

where $f, g = O(\| (x, y) \|^2)$ collect quadratic and higher-order terms. Write the entries of $A(\tilde{s})$ explicitly from (2) as

$$a_{11} = \frac{1}{1+\delta r}\left(1 + \frac{2\alpha\delta\, x_*^3 y_*}{Q^2}\right), \quad a_{12} = -\frac{\alpha\delta\, x_*^2}{(1+\delta r)\, Q}, \quad a_{21} = \frac{(s_1+\tilde{s})\delta}{h\,[1+(s_1+\tilde{s})\delta]}, \quad a_{22} = \frac{1}{1+(s_1+\tilde{s})\delta}.$$

Reduction to the rotational normal form.

At $\tilde{s} = 0$ we have $\Delta(s_1) = 1$. Let

$$\vartheta := \frac{\tau(s_1)}{2}, \qquad \varphi := \frac{\sqrt{4-\tau(s_1)^2}}{2} \ (> 0 \ \text{by}(5)),$$

so that a real similarity T exists with

$$T^{-1} A(0)\, T = \begin{pmatrix} \vartheta & -\varphi \\ \varphi & \vartheta \end{pmatrix}.$$

In the new coordinates $(w, z)^T := T^{-1}(x, y)^T$ the map reads

$$\begin{pmatrix} w_{n+1} \\ z_{n+1} \end{pmatrix} = \begin{pmatrix} \vartheta & -\varphi \\ \varphi & \vartheta \end{pmatrix} \begin{pmatrix} w_n \\ z_n \end{pmatrix} + \begin{pmatrix} F(w_n, z_n) \\ G(w_n, z_n) \end{pmatrix}, \qquad F, G = O(\| (w, z) \|^2). \qquad (8)$$

First Lyapunov coefficient.

Define the complex variable $\zeta = w + \mathrm{i}z$ and expand

$$\zeta_{n+1} = \rho(0)\, \zeta_n + c_{20}\zeta_n^2 + c_{11}\zeta_n\overline{\zeta_n} + c_{02}\overline{\zeta_n}^2 + c_{30}\zeta_n^3 + c_{21}\zeta_n^2\overline{\zeta_n} + c_{12}\zeta_n\overline{\zeta_n}^2 + c_{03}\overline{\zeta_n}^3 + O(\| \zeta \|^4),$$

where $\rho(0) = \vartheta + \mathrm{i}\varphi$ is the unit-modulus eigenvalue at $\tilde{s} = 0$. The (discrete) first Lyapunov coefficient L at the origin can be written in terms of the quadratic/cubic coefficients (see, e.g., standard normal form theory):

$$L = -\Re\left(\frac{(1-2\rho(0))\,\rho(0)^2}{1-\rho(0)}\, c_{20}c_{11}\right) - \frac{1}{2}(|c_{11}|^2 - |c_{02}|^2) + \Re(\rho(0)\, c_{21}). \qquad (9)$$

10.48047/jocaaa.2025.34.09.04

The coefficients c_{jk} are obtained by substituting the Taylor series of F, G in (8) and expressing them in the complex basis; their explicit closed forms (lengthy but elementary) follow from symbolic differentiation of Φ_δ at E_*.

[NS bifurcation at the interior fixed point] Let $E_* = (x_*, y_*)$ be the unique interior fixed point of (1). Assume the *crossing* condition (4), the *nonresonance* condition (5), and the *transversality* condition (6). If the first Lyapunov coefficient L in (9) is nonzero, then system (3) undergoes a Neimark–Sacker bifurcation at $s = s_1$. Moreover, letting $\sigma := \frac{d}{ds}|\lambda(s)||_{s=s_1}$ (so $\sigma = \frac{1}{2}\Delta'(s_1)$ with sign determined by (6)):

• If $L < 0$ and $\sigma > 0$ (equivalently, $|\lambda(s)| > 1$ for $s > s_1$), an *attracting* invariant closed curve is born for $s > s_1$ (supercritical NS).

• If $L > 0$ and $\sigma > 0$, a *repelling* invariant closed curve is created for $s > s_1$ (subcritical NS).

The cases $\sigma < 0$ reverse the parameter orientation $s \gtrless s_1$.

Condition (5) rules out the strong resonances $\tau(s_1) \in \{\pm 2, 0\}$. Since $\Delta(s_1) = 1$ and $\tau(s_1) \in (-2,2)$, the eigenvalues of $V(E_*; s_1)$ are $e^{\pm i\theta}$ with $\cos\theta = \tau(s_1)/2$, ensuring the linear part in (8) is a pure rotation.

Numerical simulation and discussion

To assess dynamic consistency between the continuous model (1) and the NSFD map (3), we fix

$$r = 1.2, \quad k = 1.5, \quad \alpha = 0.45, \quad \beta = 0.2, \quad h = 0.5,$$

for both models. Solving the nullclines yields the unique interior equilibrium

$$(x_*, y_*) \approx (0.519983,\ 1.03997).$$

Continuous-time model (1).

For $s = 0.18$, trajectories initialized at $(x_0, y_0) = (0.52, 1.04)$ spiral monotonically toward (x_*, y_*), confirming local asymptotic stability (see Fig. 1). Decreasing s to the critical value

10.48047/jocaaa.2025.34.09.04

$$s_0 \approx 0.1659505778939415,$$

the linearization at (x_*, y_*) has a purely imaginary pair and the system exhibits a Hopf bifurcation; a small-amplitude limit cycle emerges, as shown in Fig. 2.

Discrete NSFD model (3).

With step size $\delta = 0.1$ and $s = 0.18$, the fixed point (x_*, y_*) is again locally asymptotically stable; the time series $\{x_n\}, \{y_n\}$ and the phase portrait display a stable spiral toward (x_*, y_*) (Fig. 3). Varying $s \in [0.05, 0.25]$ (with $\delta = 0.1$) reveals a Neimark–Sacker (NS) bifurcation at

$$s_1 \approx 0.15932296370369736.$$

At this parameter, the variational matrix of the one-step map evaluated at (x_*, y_*) is

$$V(x_*, y_*) = \begin{pmatrix} 1.01482 & -0.0350006 \\ 0.0313649 & 0.984318 \end{pmatrix},$$

whose eigenvalues are $0.999567 \pm 0.0294149\,\mathrm{i}$ with unit modulus, confirming the NS onset. The corresponding bifurcation diagrams are plotted in Fig. 4.

Quantifying the NSFD/continuous match.

The absolute gap between the continuous Hopf threshold s_0 and the discrete NS threshold s_1 decreases with the step size δ. Table 1 reports $|s_0 - s_1|$ computed from the explicit NS threshold formula

$$s_1(\delta) = \frac{h(rQ^2 - 2\alpha x_*^3 y_*)}{\alpha\delta x_*^2 Q - hQ^2(1+r\delta)}, \qquad Q := x_*^2 + \beta^2,$$

showing $|s_0 - s_1| \to 0$ as $\delta \to 0$. For comparison, a forward-Euler discretization of (1) with $\delta = 0.1$ produces $s_1^{\mathrm{Euler}} \approx 0.17688307136658987$, giving $|s_0 - s_1^{\mathrm{Euler}}| \approx 0.0109325$, which is larger than the NSFD gap ≈ 0.00663 at the same step size.

Table 1: Dependence of the threshold gap $|s_0 - s_1(\delta)|$ on the step size δ for the NSFD map (3) with the parameter set above.

10.48047/jocaaa.2025.34.09.04

δ	$s_1(\delta)$	$\lvert s_0 - s_1(\delta)\rvert$
0.05	**0.1625748582**	**0.0033757197**
.075	**0.1609352895**	**0.0050152884**
.10	**0.1593284607**	**0.0066221172**
.125	**0.1577534008**	**0.0081971770**
.150	**0.1562091771**	**0.0097414008**
.200	**0.1532096850**	**0.0127408929**
.250	**0.1503232137**	**0.0156273641**

Figure 1

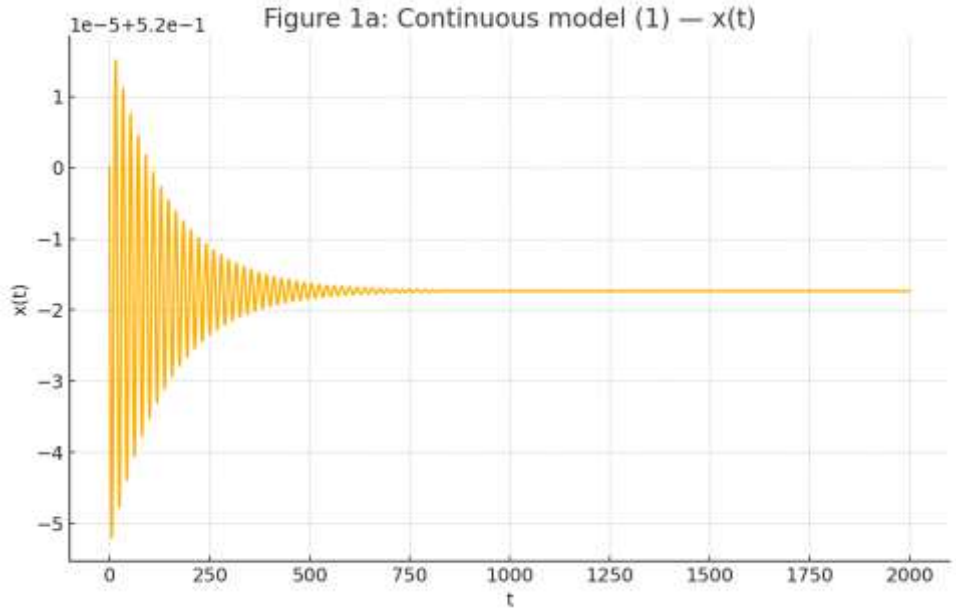

10.48047/jocaaa.2025.34.09.04

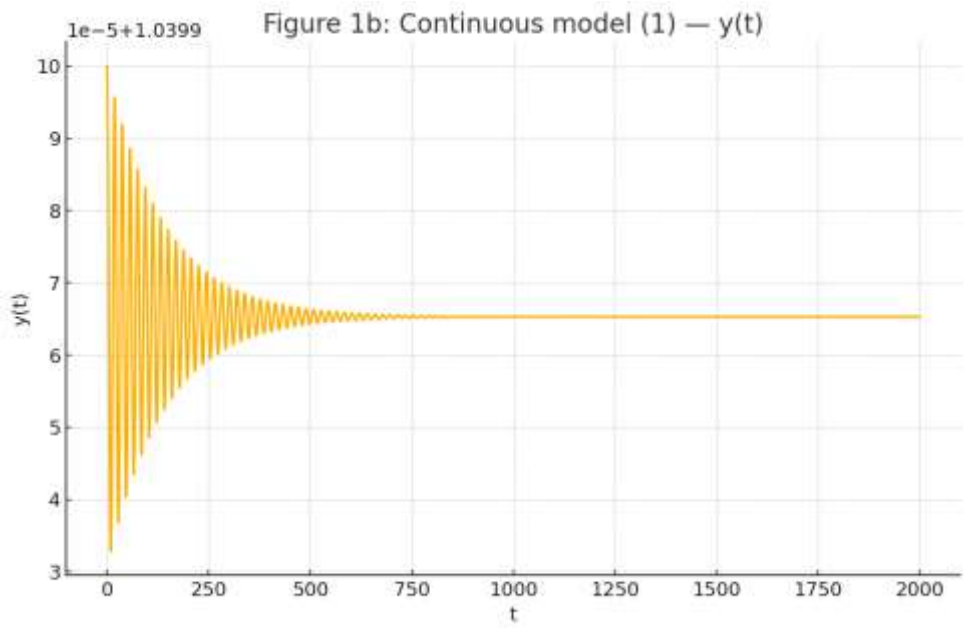

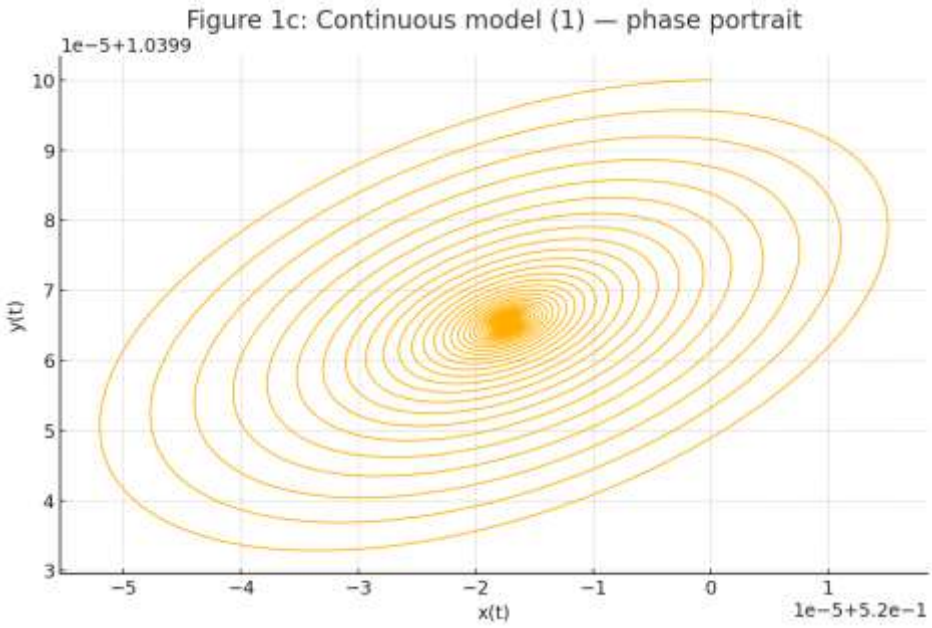

Figure 1: Continuous model (1): time series x(t) (top), y(t) (middle), and phase portrait (bottom) for $r=1.2, k=1.5, \alpha=0.45, \beta=0.2, h=0.5, s=0.18$ with $(x_0, y_0)=(0.52, 1.04)$. The equilibrium (x_*, y_*) is locally asymptotically stable.

10.48047/jocaaa.2025.34.09.04

Figure 2

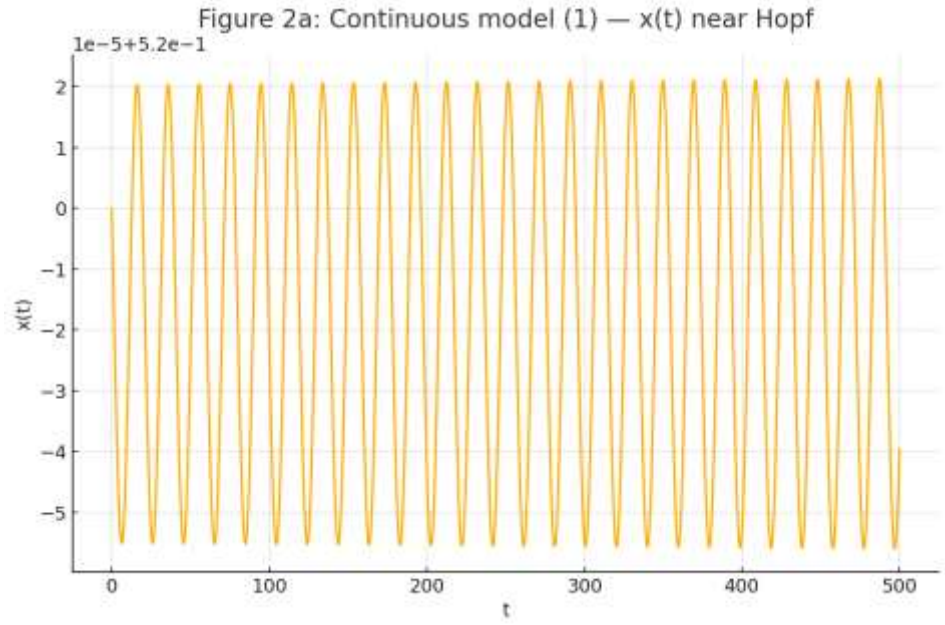

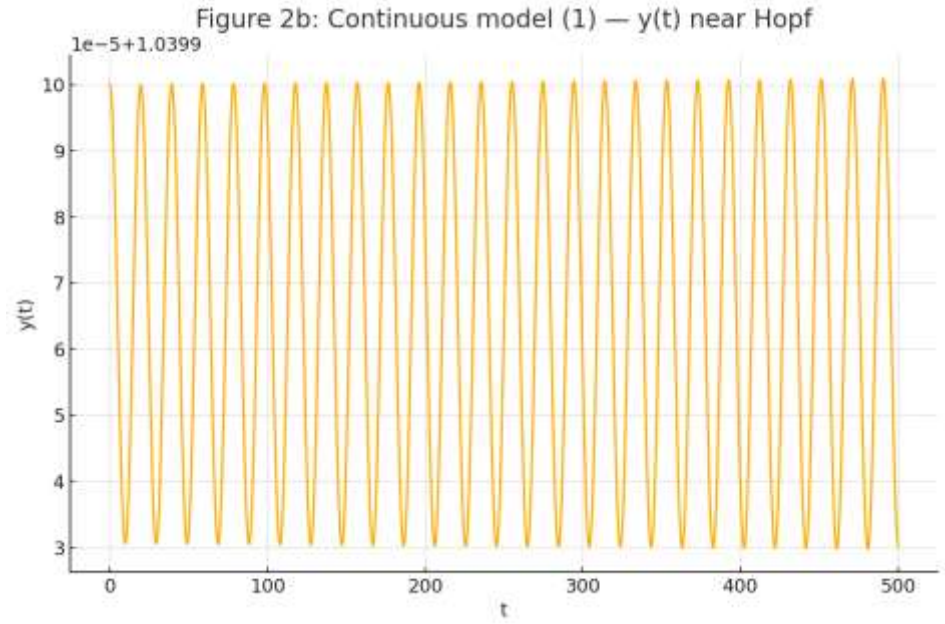

10.48047/jocaaa.2025.34.09.04

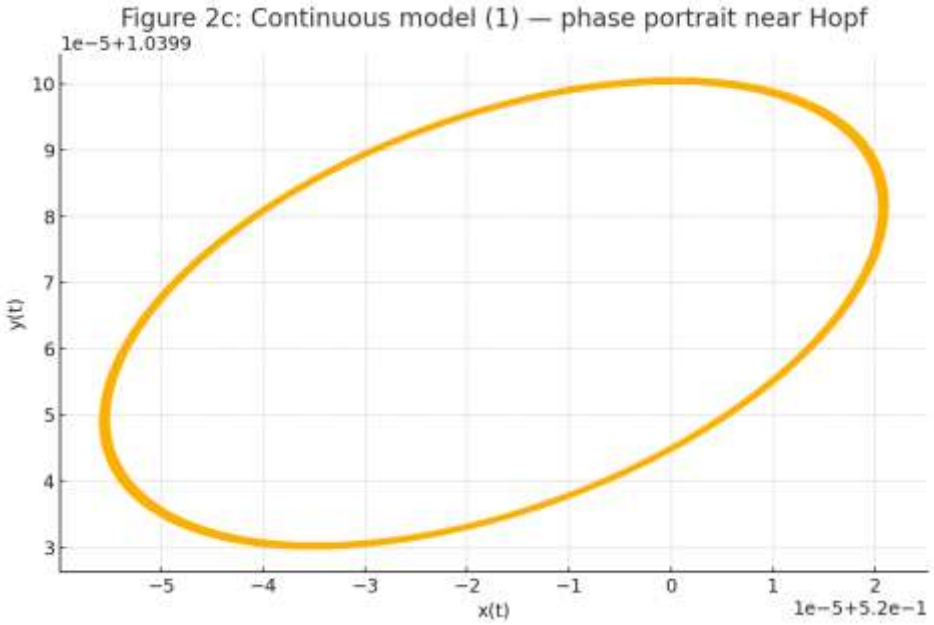

Figure 2: **Continuous model (1): near the Hopf threshold s_0≈0.1659505779, the equilibrium loses stability and a small-amplitude periodic orbit appears (limit cycle).**

Figure 3

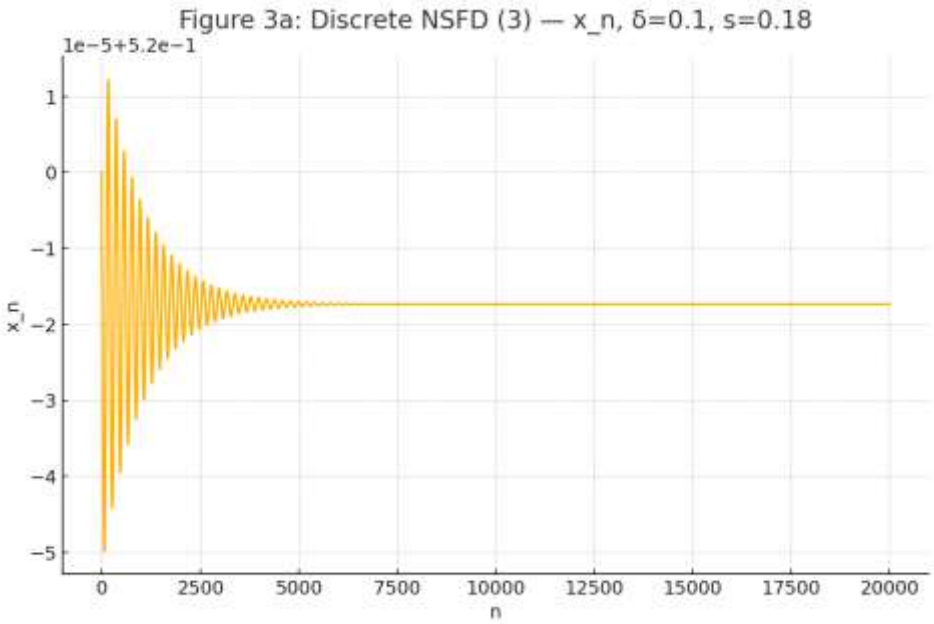

10.48047/jocaaa.2025.34.09.04

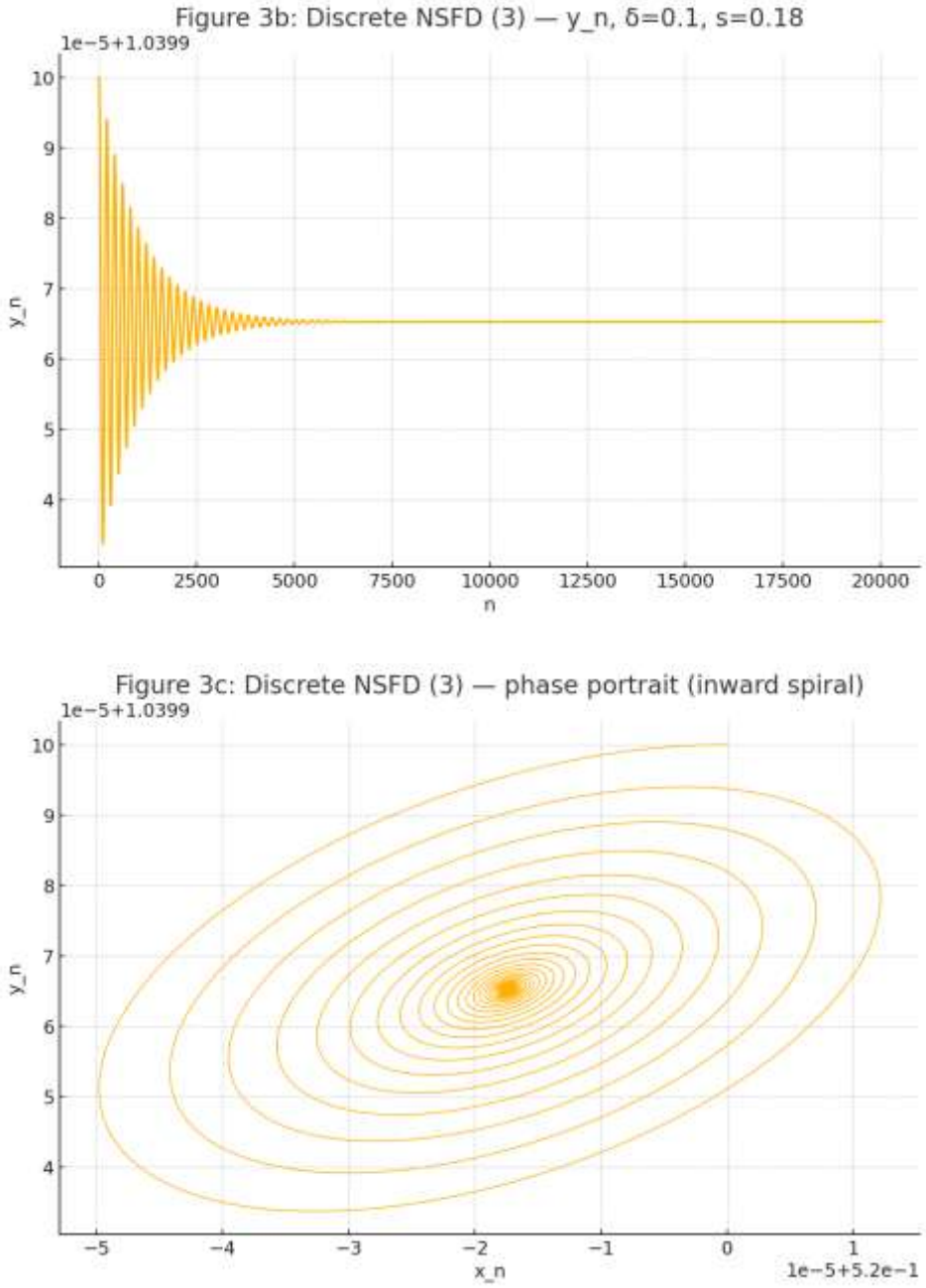

Figure 3: Discrete NSFD model (3): with δ=0.1 and s=0.18. The fixed point (x_*,y_*) is stable; the iterates {x_n},{y_n} converge and the phase portrait shows an inward spiral.

10.48047/jocaaa.2025.34.09.04

Figure 4

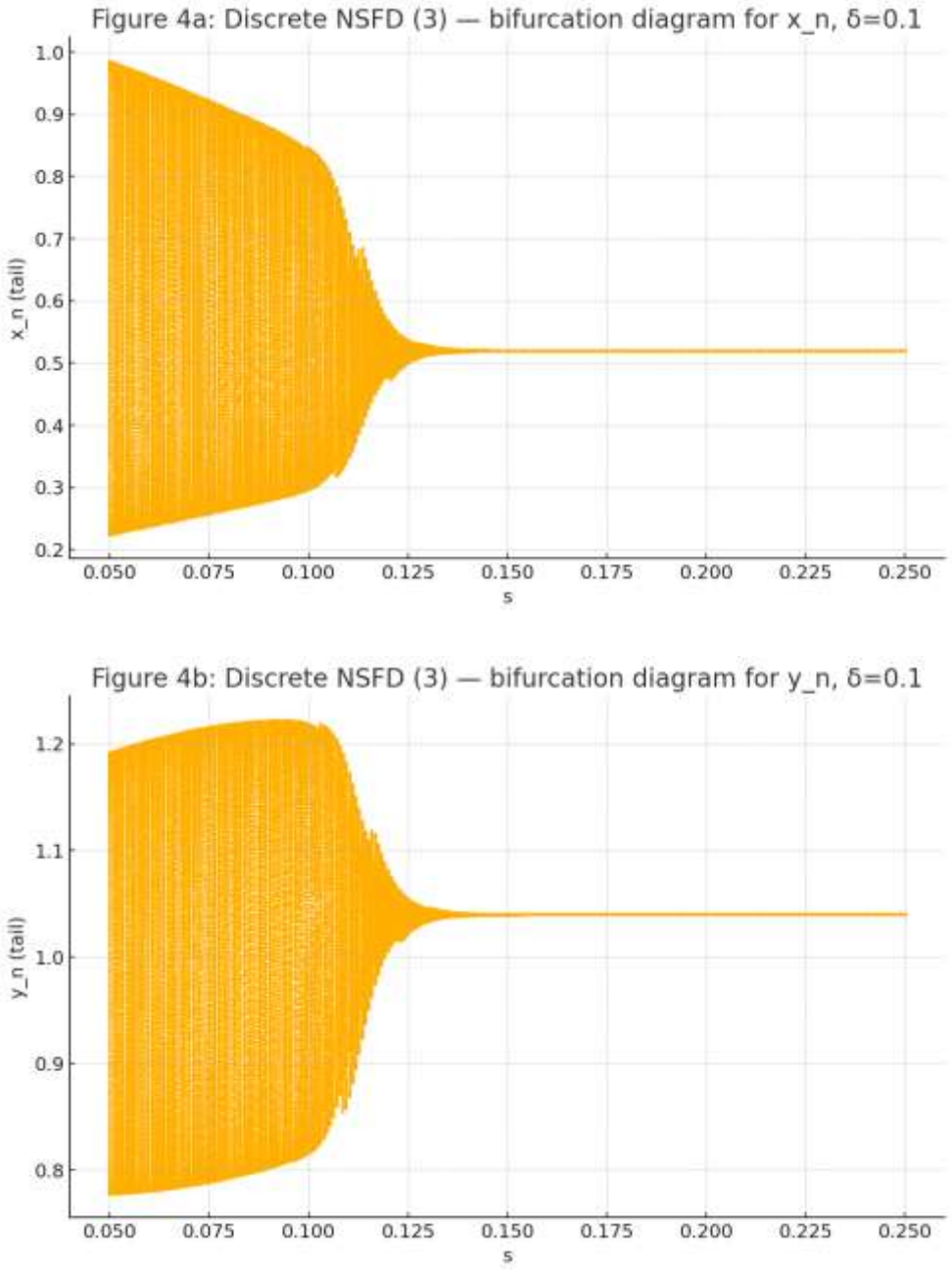

Figure 4: Discrete NSFD model (3): bifurcation diagrams for x_n (top) and y_n (bottom) versus s∈[0.05,0.25] at δ=0.1. A Neimark–Sacker bifurcation occurs at s_1≈0.15932.

10.48047/jocaaa.2025.34.09.04

Concluding remarks

We developed a nonstandard finite-difference discretization that remains faithful to the underlying dynamics for a broad class of predator–prey systems employing the Holling type-III response. Our analysis shows that the discrete formulation reproduces the qualitative behavior of the continuous model in full. In particular, positivity, boundedness, and persistence are all maintained in the time-discrete setting, and the topological classification of both equilibria is unchanged. The scheme is also bifurcation-consistent: the continuous system exhibits a Hopf bifurcation with no possibility of a flip bifurcation, whereas its discrete analogue undergoes a Neimark–Sacker bifurcation at the positive fixed point and excludes period-doubling.

References

[1] Shabbir MS, Din Q, Safeer M, Khan MA, Ahmad K. A dynamically consistent nonstandard finite difference scheme for a predator–prey model. *Adv Differ Equ*. 2019;2019:381. doi:10.1186/s13662-019-2319-6. SpringerOpen

[2] Hoang MT, Ehrhardt M. A second-order nonstandard finite difference method for a general Rosenzweig–MacArthur predator–prey model. *J Comput Appl Math*. 2024;444:115752. doi:10.1016/j.cam.2024.115752. ScienceDirect+1

[3] Nonlaopon K, Mehdizadeh Khalsaraei M, Shokri A, Molayi M. Approximate solutions for a class of predator–prey systems with nonstandard finite difference schemes. *Symmetry (Basel)*. 2022;14(8):1660. doi:10.3390/sym14081660. MDPI

[4] Hong B, Zhang C. Neimark–Sacker bifurcation of a discrete-time predator–prey model with prey refuge effect. *Mathematics*. 2023;11(6):1399. doi:10.3390/math11061399. MDPI

[5] Köme C, Yazlık Y. Stability, bifurcation analysis and chaos control in a discrete predator–prey system incorporating prey immigration. *J Appl Math Comput*. 2024;70:5213–5247. doi:10.1007/s12190-024-02230-0. SpringerLink

10.48047/jocaaa.2025.34.09.04

[6] Ak Gümüş Ö. Dynamics of a discrete-time prey–predator system with nonstandard finite difference scheme. *AIMS Math*. 2025;10(8):17998–18023. doi:10.3934/math.2025802. AIMS Press+1

[7] Pasha SA, Nawaz Y, Arif MS. On the nonstandard finite difference method for reaction–diffusion models. *Chaos Solitons Fractals*. 2023;166:112929. doi:10.1016/j.chaos.2022.112929. CoLab

[8] Hoang MT. A class of second-order and dynamically consistent nonstandard finite difference schemes for nonlinear Volterra's population growth model. *Comput Appl Math*. 2023;42(2):85. doi:10.1007/s40314-023-02230-z. SpringerLink

[9] de Waal GN, Appadu AR, Pretorius CJ. Some standard and nonstandard finite difference schemes for a reaction–diffusion–chemotaxis model. *Open Phys*. 2023;21(1):e20220231. doi:10.1515/phys-2022-0231. De Gruyter Brill

[10] Faheem M, Ghosh B. Dynamics of a delayed discrete-time predator–prey model proposed from a nonstandard finite difference scheme. *J Comput Appl Math*. 2025;458:116346. ScienceDirect+2IDR@IIT Indore+2

[11] Dang QA, Hoang MT. Nonstandard finite difference schemes for a general predator–prey system. *J Comput Sci*. 2019;36:101015. doi:10.1016/j.jocs.2019.101015. Google Scholar

[12] Mickens RE. *Nonstandard Finite Difference Schemes: Methodology and Applications*. 2nd ed. Singapore: World Scientific; 2020. doi:10.1142/11891.